ILLINOIS

UNIVERSITY OF ILLINOIS AT URBANA-CHAMPAIGN

-

PRODUCTION NOTE

University of Illinois at
Urbana-Champaign Library
Large-scale Digitization Project, 2007.

UNIVERSITY OF ILLINOIS ENGINEERING EXPERIMENT STATION BULLETIN NO. 438

Torsional Properties of Steels at High Rates of Strain

by

Paul G. Jones

Thomas J. Dolan

UNIVERSITY OF ILLINOIS BULLETIN

A REPORT OF AN INVESTIGATION

Conducted by

THE ENGINEERING EXPERIMENT STATION
UNIVERSITY OF ILLINOIS

In Cooperation With

OFFICE OF NAVAL RESEARCH
DEPARTMENT OF THE NAVY

Under
Contract N6ori-071(49)

Price: Thirty-five Cents

UNIVERSITY OF ILLINOIS BULLETIN

Volume 54, Number 47; February, 1957. Published seven times each month by the University of Illinois. Entered as second-class matter December 11, 1912, at the post office at Urbana, Illinois, under the Act of August 24, 1912. Office of Publication, 207 Administration Building, Urbana, Ill.

Torsional Properties of Steels at High Rates of Strain

by

Paul G. Jones

PROFESSOR OF THEORETICAL AND APPLIED MECHANICS

Thomas J. Dolan

PROFESSOR OF THEORETICAL AND APPLIED MECHANICS

ENGINEERING EXPERIMENT STATION BULLETIN NO. 438

ABSTRACT

An experimental study was made to determine the effects of strain rate, temperature, type of notch, and size of specimen on four steels tested in torsion. Unnotched specimens were ¼ in. in diameter and the root diameters of notched specimens were $^{3}/_{16}$ in. and ⅜ in. Two sharpnesses of notch were used giving ratios of notch radius to root diameter, r/D, of 0.160 and 0.053. Three rates of torsional strain were obtained by using angular velocities of 0.5 rpm, 27 rpm, and 1300 rpm for the flywheel which loaded the specimen. The tests were conducted at −100 F, room temperature, and 700 F.

Torque, angle of twist, and time were continuously recorded and torsional properties were determined. In general it was found that, for ranges of strain rate and temperature used, an increase in strain rate caused no appreciable change in strength but did cause a decrease in ductility and total energy absorbed. An increase in temperature caused a decrease in strength and energy that were accompanied by a decrease in ductility at low strain rates and an increase in ductility at high strain rates. There was a decrease in ultimate strength with increased size of specimen. Size effect as measured by energy considerations increased with an increase in speed and a decrease in temperature.

A study was also made of the energy conditions governing the onset of unstable fracturing.

CONTENTS

FIGURES

TABLES

I. INTRODUCTION

The behavior of a metal in many applications is influenced by factors such as the type of loading, stress distribution, state of stress, temperature, and rate of straining. In order to determine the applicability of a material for a particular service, experiments are sometimes conducted under simulated service conditions and other experiments are designed to determine the specific properties of the material which are believed to be most significant in the design. Many experiments for special applications involve high rates of straining (for example, projectile penetration measurements, deformations of metals from explosion, and various impact tests).

Tension and bending tests have been widely used to determine the influence of the various factors on the behavior of a material, and several theories have been proposed which have contributed to a better understanding of the mechanism of failure. However, it is felt that the torsion test might be significant in simulating the localized shearing actions that occur in some applications such as in the localized punching failure of an armor plate due to penetration of a projectile. The resistance of a metal to shear deformation in which high strain rates have an important influence on the mechanism of failure might be obtained from a suitably instrumented torsion test.

Measurements obtained in a rapid torsion test might be helpful in the development of a non-ballistic acceptance test for armor materials. The aforementioned localized shearing actions that occur could be simulated by the use of a small cylindrical specimen containing a circumferential groove. This would have the dual effect of increasing the effective strain rate at the root of the notch and of localizing the energy dissipation to a limited region as probably occurs in the localized complex shear fracture developed by a fragment penetrating an armor plate.

This investigation was conducted in the research laboratories of the Department of Theoretical and Applied Mechanics as a portion of the work of the Engineering Experiment Station of the University of Illinois in cooperation with the Department of the Navy, Office of Naval Research, Washington, D. C. under contract N6 ori-07149. Appreciation is expressed to the Naval Research Laboratory for their sponsorship of this project and to Dr. G. R. Irwin and Mr. J. A. Kies of the NRL for their encouragement and technical guidance of the program. Acknowledgment is due to A. P. Boresi, T. Dimoff, M. Sugi, P. Van Lierde and other research personnel who have helped with the experimental phases of this investigation.

II. SCOPE OF INVESTIGATION

In this investigation several metals were tested in torsion for various conditions of temperature, strain-rate, size of specimen, and type of notch for the purpose of determining the influence of these factors on the mechanism of failure in torsion and to determine whether such information might be helpful in the development of non-ballistic tests for armor materials. A study was also made of the elastic strain energy and the energy required for plastic deformation and crack propagation in order to have a better understanding of the conditions governing the onset of unstable fracturing of a ductile metal.

1. Materials.

Torsion tests were made on four steels which included S.A.E. 4340, S.A.E. 8727, and two steels designated as STS 065-055 and STS 065-914. Plate STS 065-055 was 1 in. thick and in previous tests had exhibited an all-fibrous fracture at one end. Specimens were cut from this end of the plate parallel to the direction of rolling. Plate STS 065-914 was 2¼ in. thick and in previous tests had

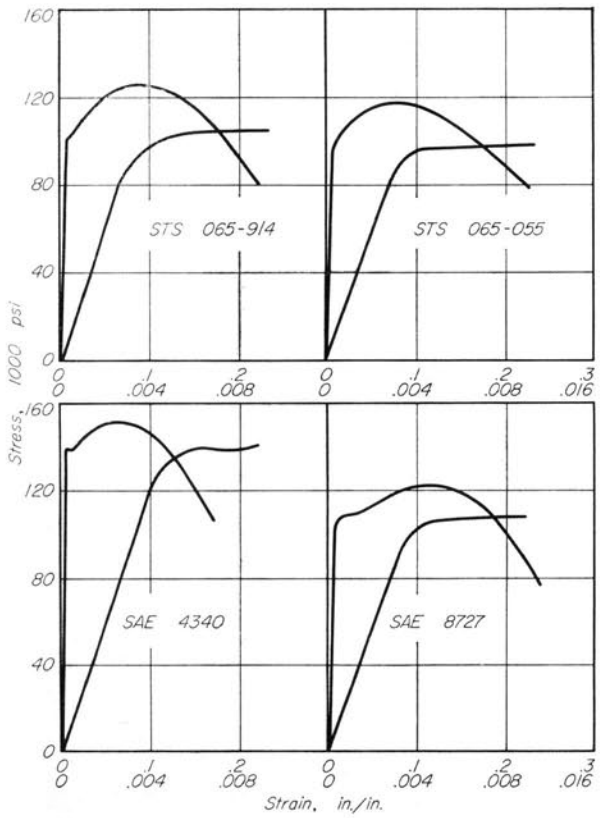

Fig. 1. Tensile Stress-Strain Curves for the Four Steels Studied (Values are average for three specimens in each case)

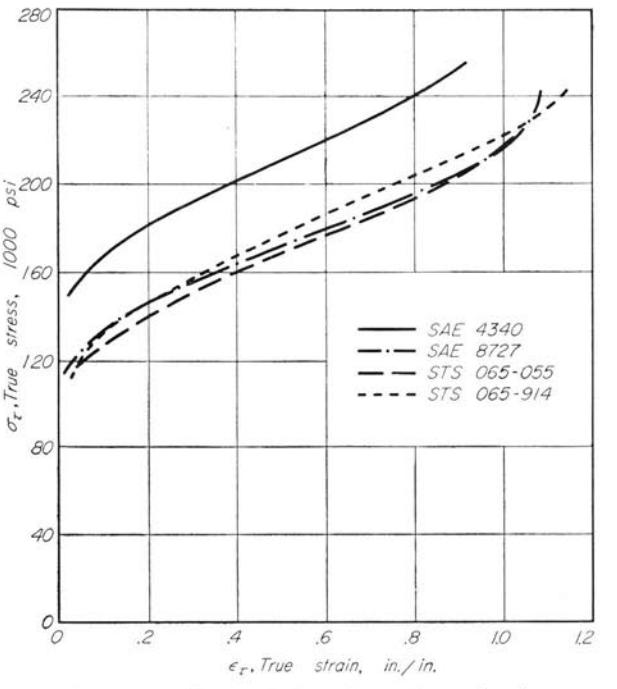

Fig. 2. Tensile "True" Stress-Strain Curves for the Four Steels Studied (Values are average for three specimens in each case)

Table 1. Chemical Composition of Steels

	C	Mn	P	S	Si	Ni	Cr	Mo	Fe
SAE 4340	0.40	0.71	0.014	0.012	0.31	1.79	0.83	0.24	rem
SAE 8727					Not Available				
STS 065-914					Not Available				
STS 065-055					Not Available				

Table 2. Static Tensile Properties

Material	Specimen Number	Yield Strength 0.2% offset psi	Yield Point (upper) psi	Yield Point (lower) psi	Ultimate Strength, psi	Elongation in one inch %	Reduction of area %
	D-70		138,300	138,300	151,500	18	60.0
S.A.E.	D-71		139,000	139,000	151,000	19	63.3
4340	D-72		142,000	139,800	151,000	18	63.3
	Average		139,800	139,000	151,200	18.3	62.2
	C-122	106,400			124,200	24	66.2
S.A.E.	C-123	105,300			122,700	21	65.4
8727	C-124	103,000			122,100	24	65.9
	Average	104,900			123,000	23.0	65.8
	A-9	100,500			124,000	24	70.1
S.T.S.	A-50	100,400			126,000	22	66.2
065-914	A-52	103,500			126,000	24	66.0
	Average	101,500			125,300	23.3	67.4
	B-48	99,500			120,000	24	69.3
S.T.S.	B-50	99,900			120,000	24	72.0
065-055	B-51	94,300			114,000	24	68.6
	Average	97,900			118,000	24.0	70.0

exhibited a heavy lamellar fracture. Specimens from this plate were cut parallel to the direction of rolling. Some were taken from the midplane of the plate and others were taken from a plane one-sixth of the plate thickness from the surface. The S.A.E. 4340 steel was received in the form of $^9/_{16}$ in. round bars and was then oil quenched and tempered to a hardness of 33 Rockwell C. Table 1 shows the chemical analysis of the S.A.E. 4340 steel. The analyses of the other steels are not available.

Average static tensile properties based on tests of three specimens $^1/_4$ in. in diameter are shown in Table 2. Average tensile stress-strain curves for each steel are shown in Figs. 1 and 2. Figure 1 shows the ordinary stress-strain curves and Fig. 2 shows the true stress-strain curves according to the following definitions:

$$\sigma = \frac{P}{A_o} = \text{ordinary stress} \qquad P = \text{load}$$

$$\epsilon = \frac{l - l_o}{l_o} = \text{ordinary strain} \qquad A_o = \text{area before loading}$$

$$\sigma_t = \frac{P}{A} = \text{"true stress"} \qquad A = \text{Actual area}$$

$$\epsilon_t = \ln \frac{A_o}{A} = \text{"true strain"} \qquad l_o = \text{original gage length}$$

l = actual length

2. Test Methods.

The geometric details chosen for the torsion test specimens are shown in Fig. 3. In order to prevent fracture of the unnotched specimens from occurring outside the one-inch gage length it was necessary to use large fillets at the ends of the reduced section and a slight reduction of diameter of the central portion. The notched specimens were of two sizes which were geometrically similar, the dimensions of the larger specimen being twice those of the smaller except for over-all length. The contour of the notches was circular at the root of the notch and two different root radii were used for each size. For the smaller specimens the root diameter was $^3/_{16}$ in. and the root radii used were 0.01 in. and 0.03 in. Thus the two root radii gave ratios of root radius to diameter of specimen at the root of the notch (r/D) equal to 0.160 and 0.053

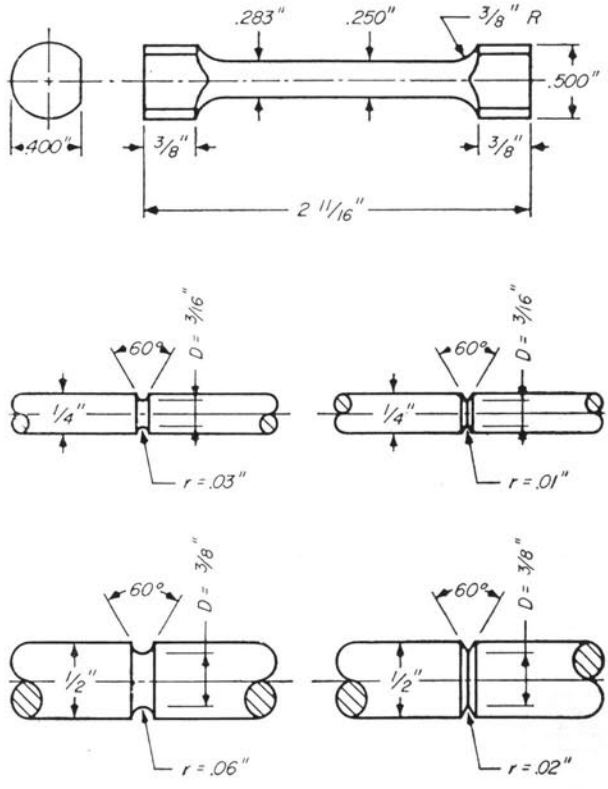

Fig. 3. Details of Torsion Test Specimens

for each size of specimen. The notches were turned in a lathe with a specially ground tool whose contour was frequently checked in an optical projection machine. The notches in these specimens were polished after machining with No. 400 grit grinding compound and a copper wire held in the chuck of a motor so that all of the polishing marks were longitudinal.

The torsion machine used in the investigation is shown in Fig. 4. A detailed description of this equipment has been previously published (1)* and only a brief discussion will be given here. A torsion specimen is attached at its right end to the torque weigh-bar W and its left end to a bar attached to the loading arm A. The flywheel F is brought to the desired speed, at which time an impulse through the solenoid S releases pins P so that they spring out to engage the loading arm. The outputs from the torque weigh-bar and the various twist measuring instruments employed were continuously recorded on photosensitive paper in a galvanometer-type oscillograph. A strain gage G is shown in place on the specimen.

Three rates of torsional strain were obtained by using angular velocities of 0.5 rpm, 27 rpm, and 1300 rpm for the flywheel which loaded the specimens. For some tests of $\frac{3}{8}$ in. diameter specimens the speed of 1300 rpm decreased about 8 percent during the tests. The other speeds used remained approximately constant during the tests. These velocities produce nominal rates of shearing strain of 0.005, 0.25, and 12.5 in. per in. per sec. respectively for unnotched specimens $\frac{1}{4}$ in. in diameter which have a length of approximately 2 in. between shoulders. The tests were conducted at −100 F, room temperature, and 700 F. The specimens tested at 700 F were heated in a furnace which enclosed the specimen and a portion of the torsion machine and were held at temperature for one-half hour before each test began. The temperature of −100 F was obtained by enclosing the specimen and a portion of the torsion machine with an insulating material (Styrofoam) and allowing the vapor from liquid nitrogen to flow into the enclosure at a rate automatically controlled to give the desired temperature. Three specimens were tested for each condition of strain-rate and temperature.

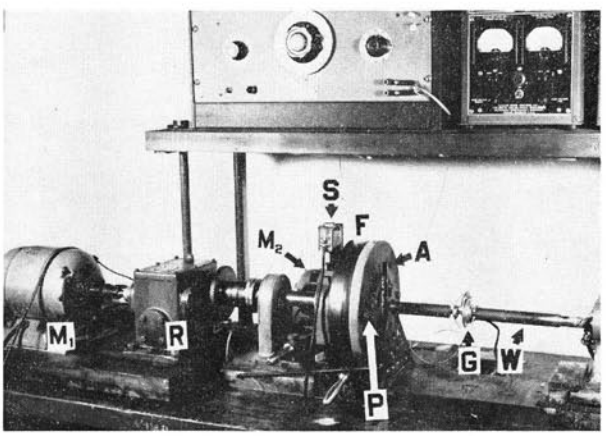

Fig. 4. Torsion Machine Arranged for Room Temperature Test at 27 rpm

* The numbers in parentheses refer to the list of references which appears on page 28.

III. EXPERIMENTAL RESULTS

The final results are plotted in graphs (Figs. 7 to 10) illustrating the variation of torsional properties with strain-rate and temperature. Each plotted point in the graphs represents the average from 3 or more tests.

The torsional properties determined in this investigation are discussed briefly in the following paragraphs.

3. Methods of Determining Torsional Properties.

In Fig. 5 is shown a typical oscillograph record of a torsion test of a notched specimen of STS 065-914 conducted at room temperature and a speed of 27 rpm. Time is represented on the horizontal axis and torque and twist are represented on the vertical axis. There are two traces representing twist as indicated on the record. The C-beam trace is used to obtain strains in the elastic region and the slide-wire trace is used for the plastic region. Simultaneous values of torque and twist obtained from this record are plotted to obtain the torque-twist curves shown in Fig. 6. The strain readings obtained from the C-beam trace are used to plot curve A, those obtained from the slide wire are used for curve B, and the measurements of flywheel twist are used to plot curve C. The torsional properties given in this report could be found for this test without the use of curve C. However, for tests made at −100 F and 700 F no strain measuring instruments other than the flywheel can be used. In order to approximate the twist of the specimen at −100 F and 700 F, a curve was plotted showing the relation between the flywheel twist and the strain instrument twist (on the 1 in. gage length) obtained at room temperature and this curve was used to obtain the twist in the 1 in. gage length for tests at −100 F and 700 F. It may be observed in Fig. 6 that the ratio of the

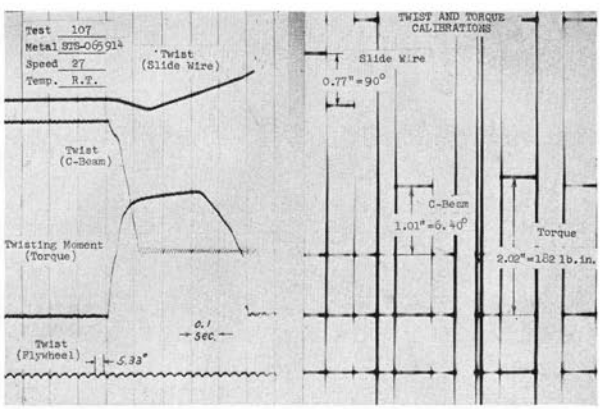

Fig. 5. Typical Oscillograph Record for Notched Specimen STS-065-914 Tested at Room Temperature and 27 rpm

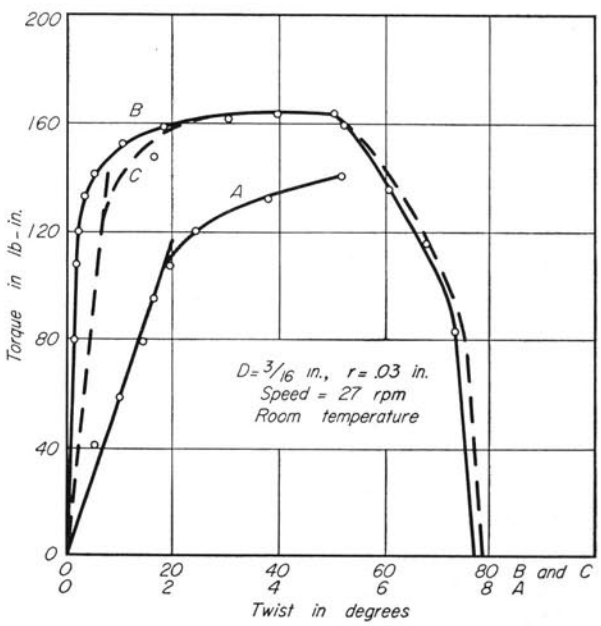

Fig. 6. Torque-Twist Diagram for STS-065-914 in Torsion (Data obtained from record shown in Fig. 5)

flywheel twist to strain-instrument twist in the elastic region is considerably higher than that ratio for total twist at the end of the test.

The modulus of rupture was computed by use of the ordinary torsion formula $\tau = Tc/J$ in which T represents the maximum torque sustained by the specimen. The shearing strain γ for unnotched specimens was computed from the angle of twist θ in radians within the gage length l and for a radius c by the relation $\gamma = c\theta/l$. No attempt was made to determine the shearing strain for notched specimens, and thus the total twist over a length of one inch including the notch is reported. For tests at room temperature the twist was obtained by use of a gage having a one inch gage length and for temperatures other than room temperature the twist was obtained from the displacement of the flywheel and conversion curves as previously explained. The values of energy absorbed by the specimens represent the total energy in in.-lb for the one in. gage length and are obtained from the area under the torque-twist diagram. For notched specimens nearly all of this energy is absorbed by the material within the notch.

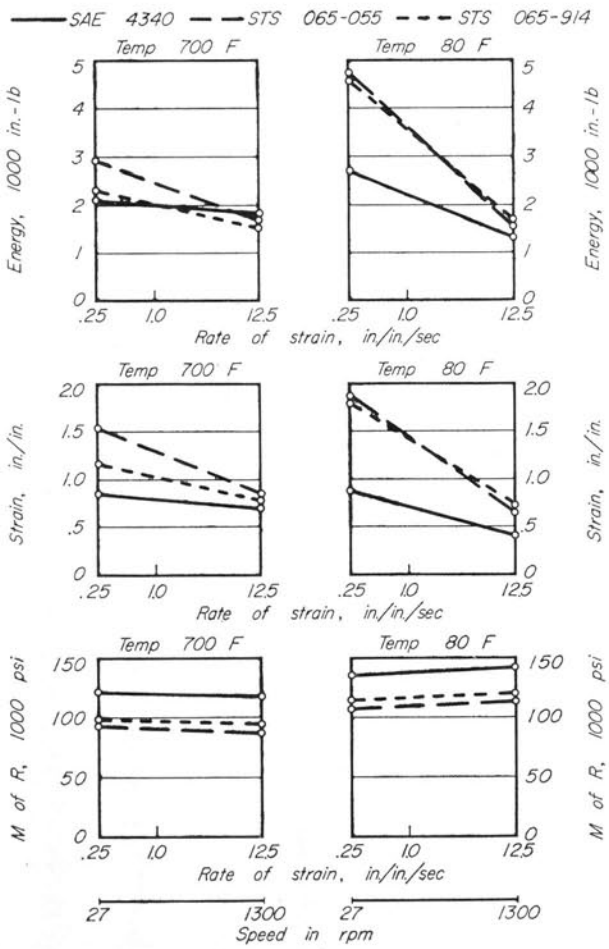

Fig. 7. Total Energy Absorbed, Shearing Strain, and Modulus of Rupture for Unnotched Specimens of Three Steels

4. Accuracies of Results.

The accuracies of the values of torsional properties reported depend on the instruments and methods used to record and interpret the data. The spread of data for a given set of test conditions is in general relatively small and this indicates good precision but not necessarily good accuracy. However it is felt that the error is less than 5 percent for values of maximum torque. Although the error in measurement of angle of twist at fracture is quite small, the twist for notched specimens under some test conditions was less than 15 degrees and the error in these readings may be somewhat greater than 5 percent.

In the study of elastic strain energy the stiffness in the elastic range was determined from strains obtained by a more sensitive gage than that used for total twist at fracture. Although the error in strain readings may be small, the strains recorded were less than one degree and the percent error may exceed 5 percent. It was found possible to repeat a stiffness determination without exceeding an error of 5 percent from the mean. However various factors which may contribute to error include slippage at the points at which the gage is attached to the specimen (especially for the $\frac{3}{16}$ in. diameter specimen) and eccentricity of loading. The percent error from the mean may not be influenced to any great extent by these factors.

5. Discussion of Results.

In the following sections will be discussed the influence of the various factors of temperature, rate of strain, specimen notch, and specimen size on the torsional properties of the four steels tested. In Figs. 7 and 8 curves are given which show the effects of rate of strain and temperature on the torsional properties.

The curves in the figures show that the trends in the behavior of the steels when subjected to the ranges of temperatures and rates of strain used are in a general way consistent with the numerous results of tension and bending tests reported by other investigators. (An excellent bibliography of such work will be found in reference (2)). Because of the many factors which influence the behavior of a material it may be found that an increased

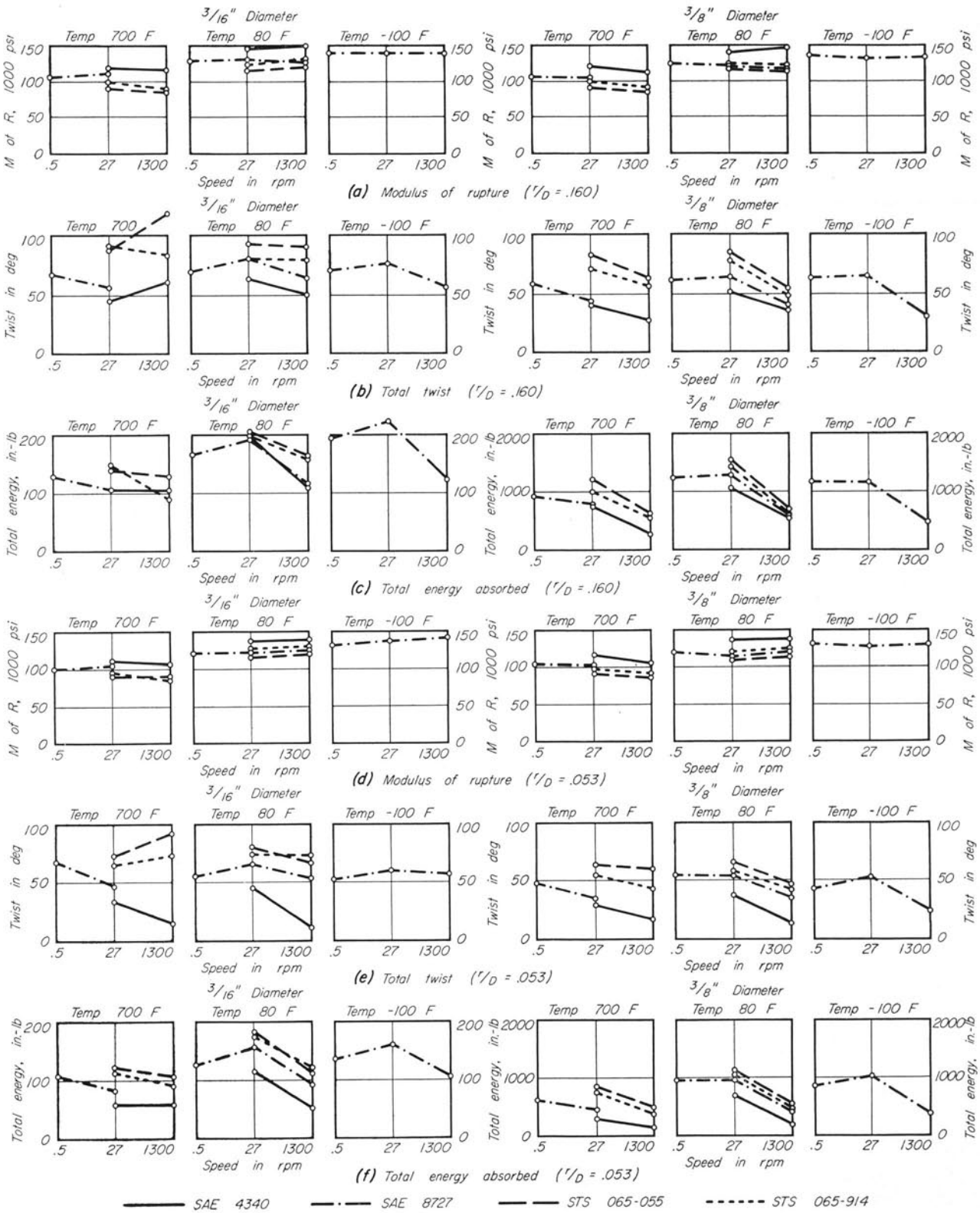

Fig. 8. Total Energy Absorbed, Total Twist, and Modulus of Rupture for Notched Specimens of Four Steels

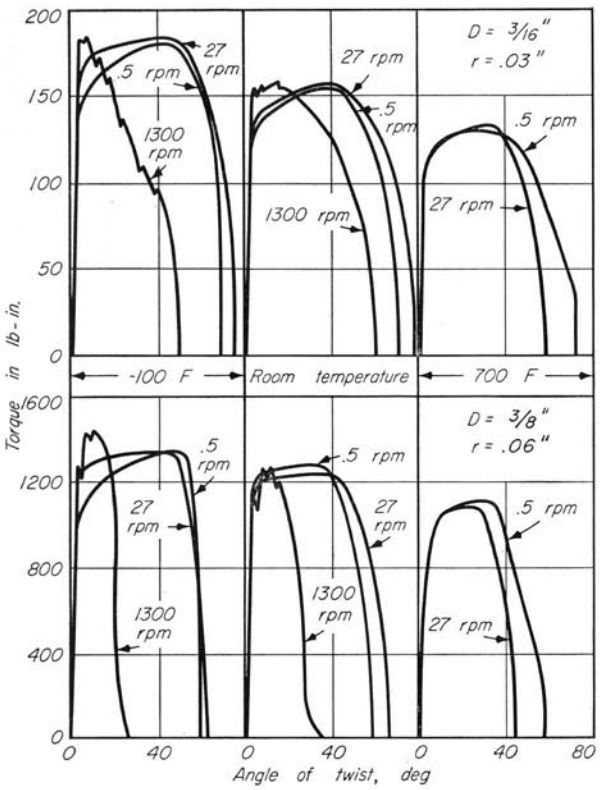

Fig. 9. Typical Torque-Twist Curves for Notched Specimens of SAE 8727

rate of strain will decrease the work to fracture (for example) in the rather limited range of temperatures used in this investigation, whereas outside that range an increased rate of strain would possibly cause an increase in work to fracture. This fact should be kept in mind when evaluating the results of this investigation.

Since the four steels behaved in a similar manner the experimental results will be discussed together in the following sections.

(a) *Effect of Temperature and Rate of Strain on Strength.*

Figures 7 and 8 show that in general an increase in temperature causes a decrease in modulus of rupture. The influence of rate of strain on modulus of rupture was negligible at all temperatures except at 700 F at which a slight decrease in strength with increased rate of strain is observed. One might expect that the strength would increase with increased rate of strain. However, it should be emphasized that the temperatures of testing indicated are those at the start of a test and that isothermal conditions could not be maintained during the test. For notched specimens the plastic deformations are so localized that a considerable rise in temperature probably takes place as the specimen is being tested. Furthermore, this rise in temperature is probably greater at the higher speeds since there would be less time for the heat to be dissipated. The effect of the increased localized temperature in weakening the specimen may have predominated over the strengthening effect that might be expected to accompany the increased rate of strain.

(b) *Effect of Temperature and Rate of Strain on Ductility.*

The curves which are given in Figs. 7 and 8 show that in general an increase in temperature resulted in a decrease in total strain at low speeds and an increase in total strain at high speeds. The S.A.E. 8727 which was the only steel tested at −100 F showed greater ductility at room temperature than at either −100 F or 700 F. In general, an increased strain-rate reduced the total deformation at rupture and the effect was greater at room temperature and −100 F than at 700 F. Tests made at 700 F on $\frac{3}{16}$ in. diameter specimens of plates STS 065-055 and STS 065-914 showed greater ductility at 1300 rpm. than at 27 rpm. The torque-twist curves for these tests were similar in shape to that for the $\frac{3}{8}$ in. diameter (r/D = 0.163) specimen of S.A.E. 8727 tested at room temperature and 1300 rpm (see Fig. 9) in which there was appreciable twist during the latter part of the test at relatively low torques. This increased the total twist at rupture without contributing to any great extent to the energy absorbed by the specimen.

(c) *Effect of Temperature and Rate of Strain on Energy.*

The total energy in in.-lb absorbed by the specimen in the one inch gage length is found from the area under the torque-twist curve. The energy is influenced not only by the maximum torque and maximum angle of twist but also by the *shape* of the torque-twist curve. Typical torque-twist curves for notched specimens of S.A.E. 8727 are shown in Fig. 9. The general shapes of the torque-twist curves for the other three steels are similar to those for S.A.E. 8727 and are not reproduced in this report. It may be seen that although an increased temperature does not cause a large change in total twist at a given speed, the average torque is decreased appreciably. Thus the total energy as measured by the area under the curve decreases with an increase in temperature. This is generally true for all four steels as may be seen from the

Table 3.

Ratio of Modulus of Rupture for Specimens Having r/D = 0.163 to Specimens Having r/D = 0.053

(Average of Three Tests)

Diam. in.	Temp. deg F	Speed RPM	STS 914	STS 055	STS 8727	SAE 4340	Diam. in.	Temp. deg F	Speed RPM	STS 914	STS 055	STS 8727	SAE 4340
		0.5	.....	.....	0.986	.....			0.5	.....	.....	1.038	.....
	−100	27	.....	.....	0.984	.....		−100	27	.....	.....	0.997	.....
		1300	.....	.....	0.989	.....			1300	.....	.....	0.968	.....
		0.5	.....	.....	1.024	.....			0.5	.....	.....	1.038	.....
3/8	RT	27	0.998	1.002	1.014	0.995	3/16	RT	27	0.985	1.003	1.035	1.032
		1300	0.956	0.998	0.987	1.022			1300	0.996	0.959	0.956	1.040
		0.5	.....	.....	1.018	.....			0.5	.....	.....	1.000	.....
	700	27	1.003	1.023	0.990	1.001		700	27	1.016	0.999	1.025	1.046
		1300	0.938	0.973	.....	1.027			1300	1.022	0.982	.....	1.083

curves which are given in Figs. 7 and 8. Figure 9 also shows that an increase in speed from 0.5 rpm to 27 rpm does not alter the shape of the curve and the energy absorbed as much as does an increase in speed from 27 rpm to 1300 rpm. For the S.A.E. 8727 steel there is an increase in energy with increase in speed from 0.5 rpm to 27 rpm for room temperature and −100 F whereas at 700 F there is a decrease in energy for a corresponding change in speed. The energy for all four steels decreased considerably when the speed was increased to 1300 rpm. This energy decrease may be seen from Figs. 7 and 8.

It may also be seen from Fig. 9 that as the speed is increased the maximum torque occurs at a lower value of twist. Since the cross-sectional area of the specimen remains approximately constant during the test it is reasonable to believe that after the maximum value is reached the load falls off because of the initiation of a crack or cracks which have started to progress through the cross-section. For tests made at 1300 rpm. it is seen that most of the total energy absorbed by the specimen is absorbed during crack propagation. A further discussion of the energy required for crack propagation will be given later.

(d) *Effect of Sharpness of Notch on Strength.*

In Table 3 is given the ratio of modulus of rupture for specimens having a ratio of root radius to specimen diameter (r/D) of 0.163 to the modulus of rupture for specimens having r/D equal to 0.053. From this table it is seen that there are about as many test conditions for which the ratio is greater than unity as those for which the ratio is less than unity and there is no consistent trend in regard to test temperature or rate of strain. It might be expected that the effect of sharpness of notch would be greater on the torque required to initiate yielding of the outer fibers than on the maximum torque, since for the elastic condition the stress concentration factor is larger for the sharper notch and for the plastic condition there may be little difference in stress concentration factor for the two notches. However, as pointed out by Dolan and Sidebottom (3) it is extremely difficult to determine the load at which yielding is initiated for a member in which a stress gradient exists such as in bending or in torsion.

(e) *Effect of Size of Notched Specimen.*

In Table 4 is given the ratio of modulus of rupture for specimens 3/8 in. in diameter to the modulus of rupture for specimens 3/16 in. in diameter. In general the modulus of rupture of the double size specimen is somewhat less than the modulus of rupture of the single size specimen which indicates a slight size effect. A comparison of curves in Fig. 8 (b and e) indicates that the large size specimen had less ductility than the small size specimen.

Size effect studies (4) have shown that if a member is loaded to fracture the work done in plastic deformation in the initial stages of the deformation is proportional to the *volume* of the material being deformed and when a crack is formed

Table 4.

Ratio of Modulus of Rupture for 3/8 in. to 3/16 in. Diameter Specimens

(Average of Three Tests)

Notch	Temp. deg F	Speed RPM	STS 914	STS 055	SAE 8727	SAE 4340	Notch	Temp. deg F	Speed RPM	STS 914	STS 055	SAE 8727	SAE 4340
		0.5	.....	.....	0.959	.....			0.5	.....	.....	1.011	.....
	−100	27	.....	.....	0.940	.....		−100	27	.....	.....	0.952	.....
		1300	.....	.....	0.967	.....			1300	.....	.....	0.946	.....
		0.5	.....	.....	0.970	.....			0.5	.....	.....	0.983	.....
r/D = 0.160	RT	27	0.996	1.075	0.937	0.959	r/D = 0.053	RT	27	0.983	0.988	0.955	0.998
		1300	0.928	0.992	0.992	0.983			1300	0.963	0.952	0.958	1.000
		0.5	.....	.....	1.04	.....			0.5	.....	.....	1.020	.....
	700	27	1.012	1.039	0.943	0.999		700	27	1.025	1.012	0.978	1.046
		1300	0.992	0.972	.....	0.954			1300	1.080	0.982	.....	1.006

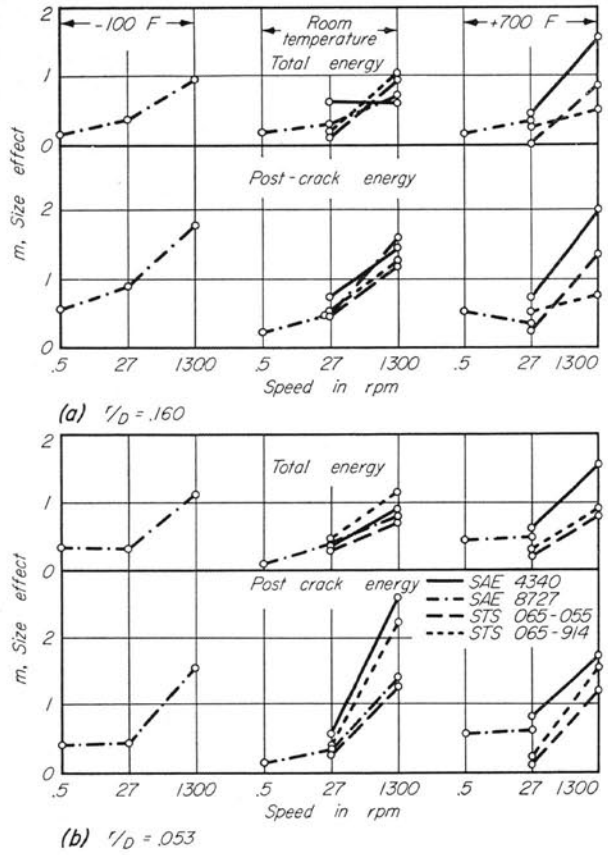

Fig. 10. Influence of Speed on Size Effect

and starts to propagate through the member, the work becomes more nearly proportional to the *area* severed. This seems to be a reasonable conclusion since the volume being deformed as the crack propagates will be confined to the vicinity of the crack itself and thus will be nearly proportional to the area of the crack and independent of the other dimensions of the member.

The notched specimens tested in the present investigation were of two sizes which were geometrically similar, the dimensions of the larger specimen being twice those of the smaller specimen. It is expected that the ratio of the energy absorbed during plastic deformation for the two sizes of specimens be about 8 and that the ratio of energy absorbed during crack propagation for the two sizes of specimens be about 4. The ratio of total energies for the two sizes will be influenced by the amount of energy for crack propagation (post-crack energy) compared with the pre-crack energy. If it is assumed that the main crack starts to propagate when the torque starts to fall off, then the torque-twist curves in Fig. 9 would indicate that in general for those tests at high speed the post-crack energy represents a larger portion of the total energy to fracture than for tests at low speeds. The energy ratio for these tests should thus be less than 8.

From experimental data obtained in bending of several ductile metals it has been shown (5) that the logarithm of the total work to fracture per unit volume is approximately linearly related to the logarithm of the specimen breadth. This relation may be expressed by the equation

$$\frac{W}{D^3} = kD^{-m} \quad \text{or} \quad W = kD^{(3-m)} \qquad (1)$$

where W is the total work to fracture in in.-lb, D is any linear dimension of the volume, and k and m are constants.

The constant m, which is the slope of the curve of log W/D^3 vs. log D, represents a measure of the size effect for the material. If the total work is proportional to the volume (D^3) of the member, then m equals zero and there is no size effect with respect to energy absorbed.

It follows from Eq. 1 that the ratio of work to fracture for two different specimens may be written:

$$\frac{W_2}{W_1} = \left(\frac{D_2}{D_1}\right)^{3-m}$$

and

$$\log \frac{W_2}{W_1} = (3 - m) \log \frac{D_2}{D_1}$$

or

$$m = 3 - \frac{\log W_2/W_1}{\log D_2/D_1} \qquad (2)$$

Eq. 2 may thus be used to evaluate m from test data on two different sizes of specimens.

Values of m have been computed by means of Eq. 2 for the two sizes of specimens used in this investigation in which $D_2/D_1 = 2$ and the results are plotted in Fig. 10 for both the total energy absorbed and the post-crack energy. In the determination of post-crack energy the crack is considered to start at the maximum torque. However, the value of twist at which the maximum torque occurs is somewhat indefinite for torque-twist curves which are fairly flat at the top. For this reason it was assumed that the crack started when the rate of decrease in torque with respect to twist reached an arbitrarily selected value of 1 lb-in./deg. for the $\frac{3}{16}$ in. diameter specimen and 8 lb-in./deg. for the $\frac{3}{8}$ in. diameter specimen. However the final results are not dependent on a critical selection of values.

The curves in Fig. 10 show that the size effect increases with an increase in speed and with a decrease in temperature. This may be interpreted to

Fig. 11. Fractured Surfaces of Notched Specimens of SAE 8727

mean that the embrittling effects of an increased speed and a decreased temperature may be much greater for large members than for small members as has been pointed out by other investigators. Also the size effect is somewhat greater for the sharper notch having r/D = 0.163. The size effect on the basis of post-crack energy (using Equation 2) is greater than that for the total energy as might be expected since the post-crack energy is less dependent on the volume of the piece than is the total energy.

(f) *Comparative Results for Plates STS 065-055 and STS 065-914.*

A comparison of torsional properties of the two special plates may be obtained from the curves which are given in Figs. 7 and 8. In general there is little difference between the results obtained for the two steels. Plate 065-914 has consistently higher strength values, lower ductility, and lower energy than Plate 065-055 but the differences are not large.

However, results of tests on small specimens may not be sufficient to predict the behavior of a large plate unless consideration is given to size effect. Possibly the best differentiation with respect to the ability of a large plate to resist projectile penetration may be obtained from a study of size effect for the two materials. In Fig. 10 it is seen that (except for tests made on specimens having r/D = 0.160 at 700 F and 1300 rpm) the size effect for Plate 065-914 is consistently higher than that for Plate 065-055. It is felt that this difference in size effect is significant and that a large plate from STS 065-914 would probably be less able to resist projectile penetration than STS 065-055.

(g) *Effect of Location of Specimen in Plate 065-914.*

Some specimens of Plate 065-914 were taken 1/6 the plate thickness from the surface and others were taken from the midplane of the plate. A comparison was made of the results for specimens from the two locations and it was concluded that the difference in behavior was no larger than might be expected from the spread of data for any given set of test conditions.

(h) *Fracture Characteristics for the Four Steels.*

Fracture of a torsion specimen occurs without an appreciable change in its diameter or length. Usually a ductile material will exhibit a sharp clean break in a plane which is perpendicular to the axis of the specimen, although in some instances unnotched ductile specimens at low temperature have broken on planes of longitudinal shear (6). Fracture of brittle materials such as gray cast iron in torsion will fail in tension at approximately 45 degrees to the transverse plane.

All of the specimens tested in this investigation failed on a transverse plane and photographs of typical fractured surfaces for S.A.E. 8727 are shown in Fig. 11. The fractured surfaces of the other steels are similar in appearance to those of S.A.E. 8727 and photographs of fractured surfaces of these steels are not included in this report. The rubbing surfaces of the broken specimen after rupture may have changed the appearance of the fractured surface to some extent. The direction of twist was such that the torque applied to the surface shown was clockwise. The speed of testing has a great influence on the general appearance of the fractured surface. The test results indicate that in general the ductility at low speed is higher than at high speed. The smooth appearance of specimens tested at 1300 rpm indicates this difference in ductility. It would appear that in tests at 27 rpm and 0.5 rpm cracks originate at a number of different points at or near the periphery of the specimen. These cracks join up to form a main crack which progresses toward the center of the specimen, apparently terminating at the dark spot observed in each of the fractured surfaces. For specimens tested at high speeds it would appear that either the main

crack is initiated at or near the surface without the accompanying scattered nuclei of initial cracks or that the initial cracks which form are not accompanied by the plastic deformation which gives rise to the markings shown in specimens fractured at low speeds.

In some of the tests on the 3/8 in. diameter specimen at high speed, the main crack progressed very rapidly once it was initiated and as a result the torque trace on the oscillograph record dropped so rapidly that the photographic paper could not record the descending trace. When this occurred at high speeds the sudden drop in torque was from the maximum torque to zero torque. However, for low speed tests there was always a considerable rounding off of the torque time trace before the torque suddenly dropped to zero. It may be that the initial cracks which formed near the surface were responsible for the rounding off of the curve and once the main crack formed, its progression was very rapid causing the torque to drop suddenly to zero. Evidence that considerable twist occurred in some of the tests after the cracks had appeared at the surface was found when measurements of final twist were made after the specimen was removed from the machine. These measurements which were obtained by fitting the specimen together at the periphery were always less than the twist recorded on the oscillograph record by the twist-measuring instruments used.

IV. ENERGY REQUIREMENTS FOR SELF-PROPAGATION OF A CRACK

One of the earliest attempts to explain crack phenomena was made by Griffith (7) in 1920. Griffith assumed that a crack arising from a defect (so-called Griffith's crack) would grow when the required energy needed in the formation of the new surface is less than the liberated strain energy due to the spread of the crack. This concept provides a convenient mechanism by which it is possible to explain why under certain stress conditions certain defects in the metal will grow to dangerous size and ultimately cause fracture.

It has been pointed out (8) that the Griffith theory does not apply to the problem of fracture of metals because the original theory does not allow for plastic deformation while actually some plastic deformation always accompanies fracture in metals. To circumvent this difficulty some authors have interpreted the energy needed in the formation of new surfaces to mean not only surface energy as originally envisioned by Griffith, but also the much larger quantity of energy needed for plastic deformation of material adjacent to the newly formed surface. In a recent paper (9) by Irwin and Kies this approach was used in a study of the mechanical concepts basic to an understanding of unstable fracturing* of large welded structures and to notched-bar fracture tests conducted in slow bending. In the present report this approach will now be extended to the problem of fracture tests in torsion.

In Fig. 12 is shown a schematic diagram of a torque-twist curve for a notched specimen in torsion in which T represents the torque applied to the specimen and θ represents the twist over an arbitrary length of the specimen including the notch. The twist, θ, for any point such as E is considered to consist of plastic or irrecoverable twist, θ_p, and elastic or recoverable twist, θ_e. If the load is released at point E the curve is assumed to follow the straight line ED. The torsional stiffness M of the specimen at this point is expressed by the equation

$$M = \frac{T}{\theta_e} \tag{3}$$

and the elastic strain energy, E, is represented by the area of the triangle DEF. For an increment of twist $\Delta\theta$ the principle of work and energy gives the following equation:

$$T\Delta\theta - \Delta E - \Delta W = \Delta K$$

where W is the dissipated energy or irrecoverable energy required for plastic deformation and crack propagation; K is the kinetic energy; and T, θ, and E are as previously defined. For conditions prior to unstable, fast-fracturing the kinetic energy K may be considered negligible and in the limit as $\Delta\theta$

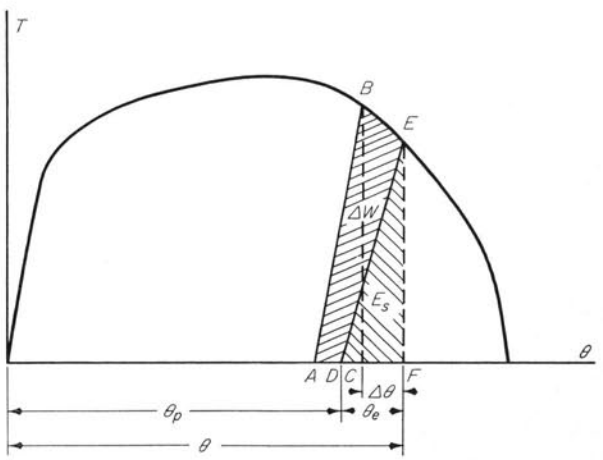

Fig. 12. Schematic Diagram of Torque-Twist Curve in Torsion

* The term "unstable fracturing" is used in this report to designate a sudden type of fracture in which the energy needed for crack propagation is supplied from the elastic strain energy of the specimen and the members to which it is attached.

approaches zero we may write

$$T\frac{d\theta}{dA} - \frac{dE}{dA} = \frac{dW}{dA} \tag{4}$$

where A is the area of the cracked surface. (In this report the cracked surface is considered to include the area of lateral cross-section of the original notch although this added constant will not influence the final conclusions.) Since $\theta = \theta_p + \theta_e$ the preceding equation may be written

$$T\frac{d\theta_p}{dA} + T\frac{d\theta_e}{dA} - \frac{dE}{dA} = \frac{dW}{dA} \tag{5}$$

The elastic strain energy is represented by the area of the triangle DEF. Thus

$$E = \frac{1}{2}T\theta_e \tag{6}$$

which with equation 3 becomes

$$E = \frac{1}{2}M\theta_e^2 \tag{7}$$

It perhaps should be pointed out that because of residual or "locked in" elastic stresses which are not recoverable when the external torque is released, the area of the triangle DEF will not represent completely the elastic strain energy E. If Eq. 7 is differentiated with respect to A we obtain

$$\frac{dE}{dA} = \frac{1}{2}M \cdot 2\theta_e\frac{d\theta_e}{dA} + \frac{1}{2}\theta_e^2\frac{dM}{dA}$$

Since

$$\frac{d\left(\frac{1}{M}\right)}{dA} = -\frac{1}{M^2}\frac{dM}{dA} \quad \text{and} \quad T = M\theta_e,$$

then

$$\frac{dE}{dA} = T\frac{d\theta_e}{dA} - \frac{1}{2}T^2\frac{d\left(\frac{1}{M}\right)}{dA}$$

and

$$T\frac{d\theta_p}{dA} + \frac{1}{2}T^2\frac{d\left(\frac{1}{M}\right)}{dA} = \frac{dW}{dA} \tag{8}$$

The Griffith condition which requires that there be no plastic deformation, θ_p, will be satisfied if

$$\frac{1}{2}T^2\frac{d\left(\frac{1}{M}\right)}{dA} = \frac{dW}{dA}.$$

In order to study the conditions governing the onset of unstable fracturing in torsion an experimental investigation was made to determine the values of the fracture work rate, dW/dA, and the elastic strain energy release rate dE/dA. This study is complicated by the fact that the notch depth, x, and consequently the lateral area of the crack, A, is unknown for corresponding values of T and θ. In other investigations methods of staining have been used to determine the cracked area for loads in bending where the crack opens up and allows the stain to penetrate to the bottom of the crack. This method did not appear feasible in the torsion tests and a method was used which involves a concept of "equivalent" notch depth for precracked specimens. This method is discussed in the next paragraphs.

In order to determine the stiffness of a specimen having a circumferential crack as a function of the depth of the crack, a series of tests were made on steel specimens having notches of various depths. The notches were made by use of a sharp lathe tool after which the notch depth was increased about 0.01 in. by use of grinding compound and a copper wire whose radius was 0.003 in. The stiffness of a notched specimen is obviously dependent on the notch radius used. However it is the rate of change in stiffness with respect to notch depth that is desired. It is felt that this rate of change will be more or less independent of the notch radius for fairly sharp notches.

The experimental results of notch stiffness for two sizes of specimens are shown in Fig. 13 in which the reciprocal of notch stiffness (compliance) is plotted against the notch depth. The slopes of the curves for various notch depths were obtained from Fig. 13 and values of $\frac{d(1/M)}{dA}$ were computed. In Fig. 14 these values are plotted against A/A_o where A represents the lateral area of the crack (from the outer diameter) and A_o represents the original area of the specimen. Values of the ordinates, $\frac{d(1/M)}{dA}$, in Fig. 14 may be used in Eq. 4 to compare with dW/dA to be obtained later.

Equation 4 expresses the relation between the external work rate $T\frac{d\theta}{dA}$, the rate of release of elastic strain energy, dE/dA, and the fracture work rate dW/dA. For conditions of unstable, fast fracturing the work done by the external torque will be zero and fracture will occur with work rate values dW/dA equal to or less than the release rate of elastic strain energy. A series of torsion tests were made on notched specimens of three steels for the purpose of determining the nearness of the equality of dW/dA and dE/dA and consequently the near-

ness to onset of fracture instability. These tests will now be described.

Torque was slowly applied to each specimen tested until a point was reached at which the torque started to decrease from the maximum or ultimate torque. The torque was quickly released to zero and slowly reloaded and a record on the oscillograph was obtained of torque and twist until the release torque was once more attained. An increment of twist was applied to the specimen after which the torque was again suddenly released and the process was repeated.

In Fig. 12 the torque-twist curve can be traced as follows. If the torque is released at point B the curve will follow the line BA to A. On increase of torque the curve follows the line AB back to point B. A further increment of twist gives the curve BE and on release of torque the curve follows ED to point D. On increase of torque the curve follows line DE back to E, etc. In some of the tests the torque on reloading did not quite attain the magnitude of the release torque; however, the differences were not more than a few percent.

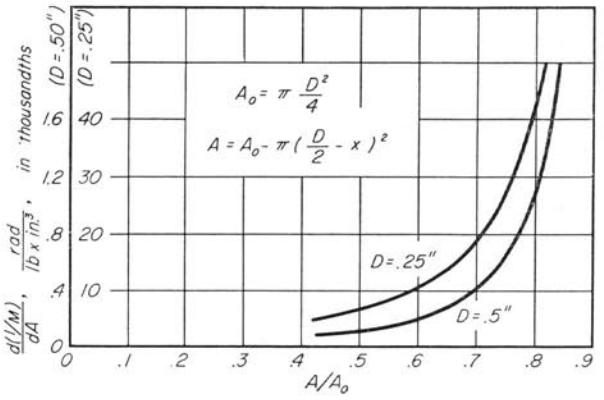

Fig. 14. Rate of Change in 1/M for Notched Specimens of SAE 4340

For each specimen tested the torque was released and the specimen reloaded about four times before fracture occurred. Torque-twist curves were plotted from the data obtained and the stiffness for each unloading program was computed. In some of the tests torque and twist data were obtained for the unloading part as well as the loading part of the cycle. Stiffness determinations for unloading

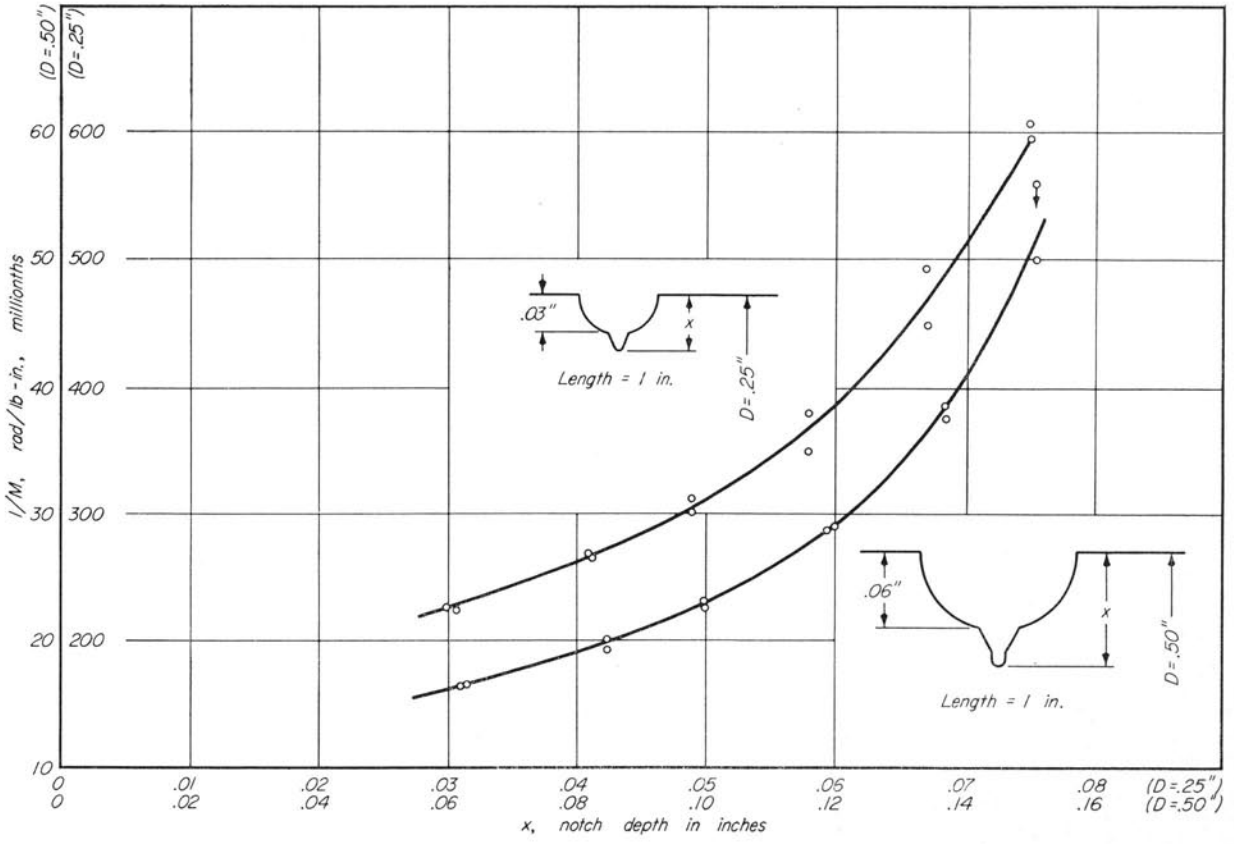

Fig. 13. Notched Specimen Stiffness of SAE 4340

did not differ appreciably from those for loading and because of convenience of instrumentation, twist data were obtained only for load increase. Four specimens for each of two sizes were tested for each steel.

The stiffnesses obtained from the unloading program were used to determine equivalent notch depths, x_e, from Fig. 13. Since the notch radius for the data in Fig. 13 is considerably greater than that for the progressing sharp notch of the specimen, the equivalent notch depth is probably less than the actual depth. However, we are interested in rates of change rather than absolute values so the error introduced may not be large. Having found equivalent notch depths the torque at load release is now plotted against the equivalent notch depth in Fig. 15 for the two sizes of specimens. Each curve represents the average of data obtained from four similar specimens and each plotted point represents data for one load-release cycle. We now have average values of equivalent notch depth for any torque imposed on the specimen as the notch progresses through the specimen. These values will be used in computing $T\frac{dA}{d\theta}$ but we must first find a relation between θ and A.

For the release torques from the unloading program, average values of equivalent notch depth, x_e,

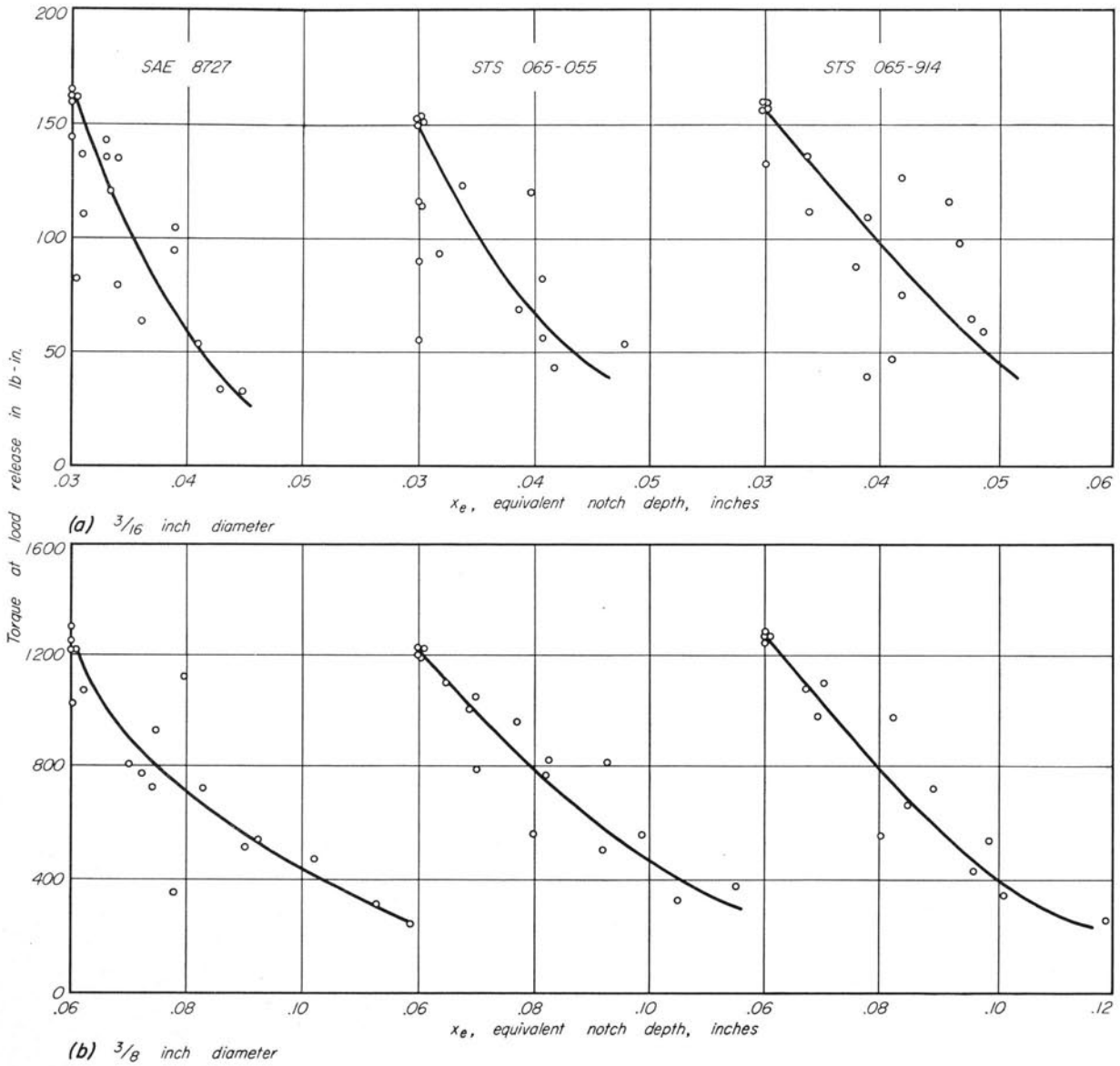

Fig. 15. Equivalent Notch Depths at Load Release for 3/16 in. and 3/8 in. Diameter Specimens

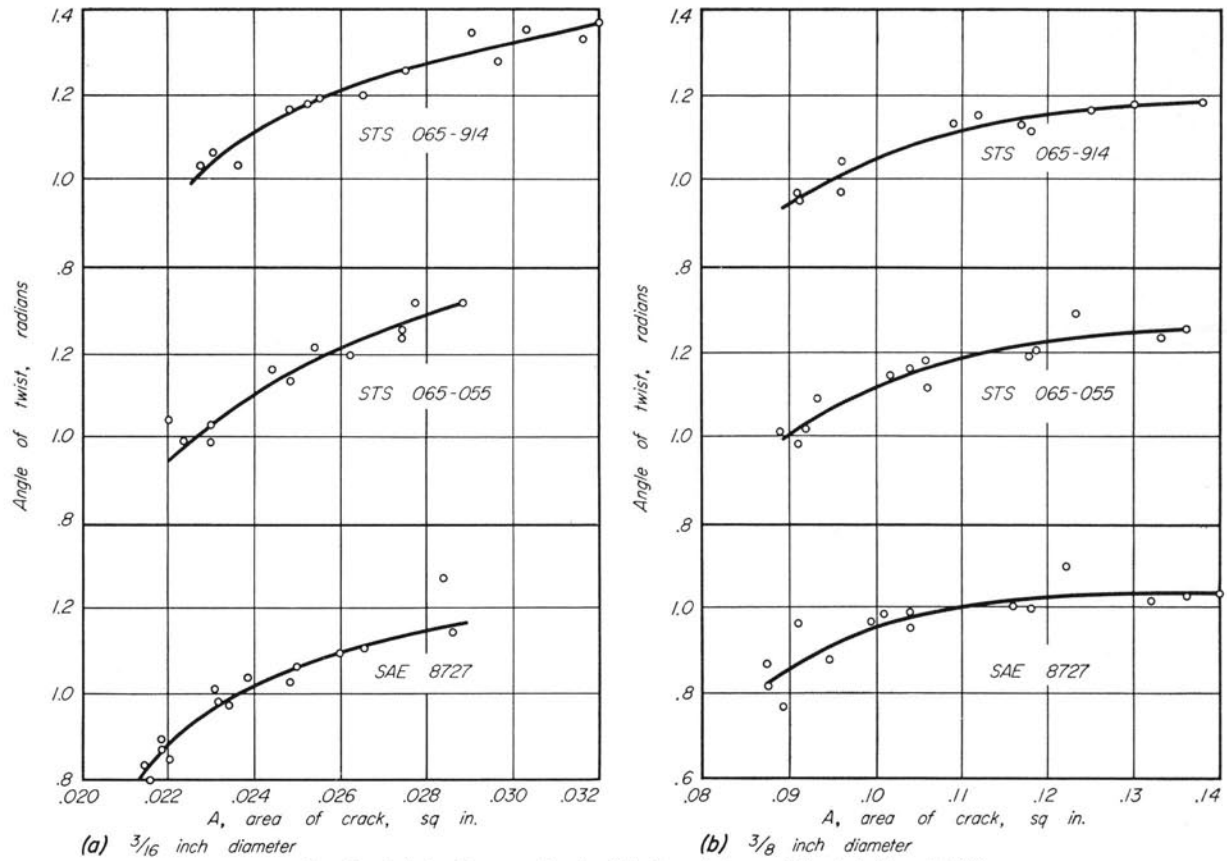

Fig. 16. Relation Between Angle of Twist and Area of Crack (r/D = 0.160)

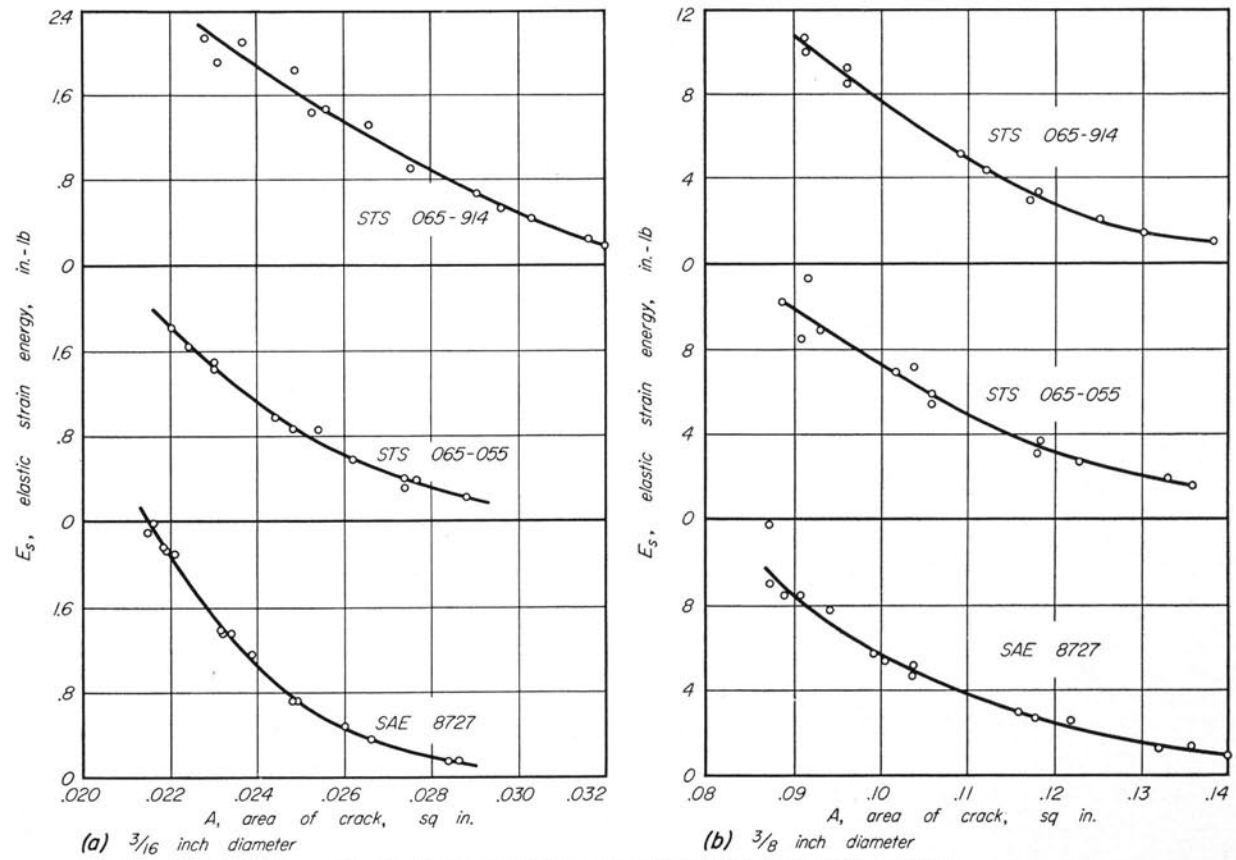

Fig. 17. Elastic Strain Energy for Notched Specimens (r/D = 0.160)

are obtained from Fig. 15 and the notched area A is computed from the equation $A = A_o - \pi \left(\frac{D}{2} - x_e\right)^2$ where $A_o = \frac{\pi D^2}{4}$ and D represents the overall diameter. In Fig. 16, test values of total twist, θ, are plotted against these values of A. The slope $d\theta/dA$ is obtained from Fig. 16 using arbitrary values of A (or x_e) and the values of $T\frac{d\theta}{dA}$ are computed.

It is now desired to find dE/dA. The elastic strain energy E is found from the equation $E = \frac{1}{2} T^2 (1/M)$ using test values of T and (1/M) and the curves of E vs. A are drawn in Fig. 17. From these curves the slopes dE/dA are obtained for the arbitrary values of A selected for use in determining $T\frac{d\theta}{dA}$. The fracture work rate dW/dA may now be computed from Eq. 4.

Fig. 18 shows the variation in dW/dA and dE/dA with increasing notch depth as measured by the ratio A/A_o. Values of dW/dA are seen to be considerably greater than the elastic strain energy release rate dE/dA for that portion of the torque-twist diagram considered. Thus in order that fracture continue it is necessary to supply external energy at the rate $T\frac{d\theta}{dA}$. Self-fracturing or the ability of the crack to progress on the release of elastic strain energy alone will not occur until the curve for dW/dA reaches the level of the corresponding curve of dE/dA.

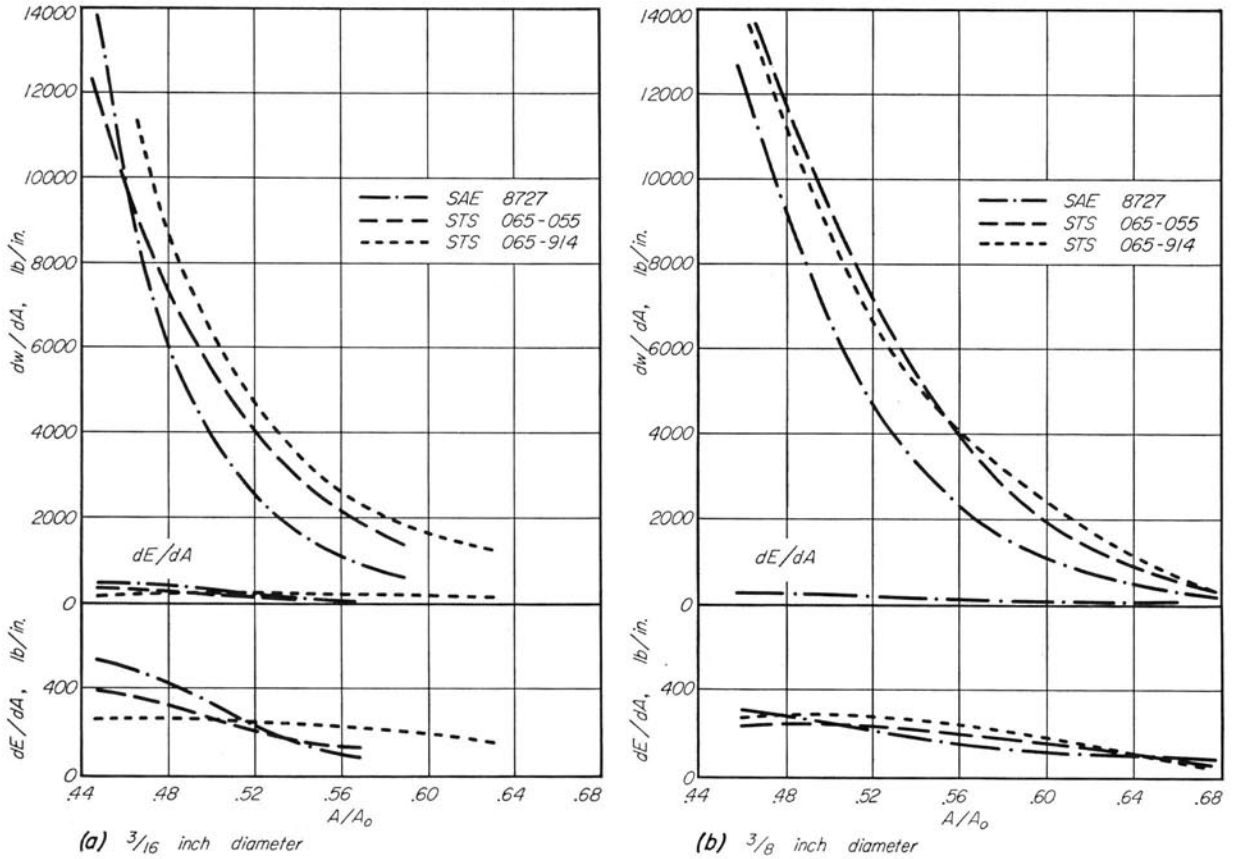

Fig. 18. Ductile Fracture Work Rates and Strain Energy Release Rates for Notched Specimens (r/D = 0.160)

V. SUMMARY AND CONCLUSIONS

An experimental study was made on four steels to determine the effect of rate of strain, temperature, sharpness of notch, and size of specimen on the mechanical properties in torsion. Unnotched and notched round specimens were tested in torsion at −100 F, room temperature, and 700 F using nominal rates of twist of 0.5 rpm, 27 rpm, and 1300 rpm. Values of torque, angle of twist, and time were continuously recorded automatically to provide data from which the torsional properties were computed.

A study was also made of the elastic strain energy and the energy required for plastic deformation and crack propagation in order to have a better understanding of the conditions governing the onset of unstable fracturing.

An analysis of the experimental data was made and the following conclusions are summarized.

1. For the ranges of temperatures and rates of strain used in the tests an increase in temperature caused a decrease in modulus of rupture and total energy to fracture. In general, maximum shearing strain at rupture decreased at low speeds and increased at high speeds.

2. An increase in rate of strain caused no appreciable change in modulus of rupture but caused a decrease in total strain and energy.

3. An increase in sharpness of notch had a negligible effect on the strength of the four steels but increased the size effect as based on total energy and post-crack energy.

4. The effect of increasing the dimensions of the notched specimens by a factor of 2 was to cause a slight decrease in strength and ductility. Size effect as measured by the criterion of energy increased with an increase in speed and a decrease in temperature. The size effect is greater for the sharper notch and is greater for post-crack energy than for total energy.

5. A comparison of results for the two STS plates indicates little difference in strength, ductility, or energy absorbed. However, size effect is higher for Plate STS 065-914 and it is felt that this may be significant in indicating that a large plate made from this steel would be less able to resist projectile penetration than from STS 065-055.

6. The study of the energy requirements for self-propagation of a crack indicates that unstable fracturing should not be expected for these tests.

VI. REFERENCES

1. "Application of Experimental Stress Analysis to Torsion Research," by C. E. Work and T. J. Dolan, Proc. Exp. Stress Analysis, Vol. 12, No. 1, pp. 79-90 (1954).

2. "The Influence of Temperature and Rate of Strain on the Properties of Metals in Torsion," by C. E. Work and T. J. Dolan, University of Illinois Eng. Exp. Station, Bulletin No. 420 (1953).

3. "Raised Yield Point in Bend Tests," T. J. Dolan and O. Sidebottom, Metals Progress, Vol. 50, No. 4, pp. 653-657, October 1946.

4. "On the Characteristics of Notched-Bar Impact Tests," by T. E. Stanton and R. G. C. Batson, Proc. Inst. Civil Eng., Vol. 21, p. 67 (1920).

5. "The Effect of Size on Fracturing," by G. R. Irwin, Proc. Am. Soc. for Testing Matls., Vol. 54, pp. 176-194 (1954).

6. "An Experimental Study of the Influence of Various Factors on the Mode of Fracture of Metals," by P. G. Jones and W. J. Worley, Proc. Am. Soc. for Testing Matls., Vol. 48, pp. 648-663 (1948).

7. "The Phenomenon of Rupture and Flow in Solids," by A. A. Griffith, Phil. Trans. Royal Soc. of London (1920).

8. "Energy Criteria of Fracture," by E. Orowan, The Welding Journal, Research Supplement, Vol. 20, No. 3, pp. 157-160 (1955).

9. "Critical Energy Rate Analysis of Fracture Strength," by G. R. Irwin and J. A. Kies, The Welding Journal, Research Supplement (April 1954).

3050—2-57—59980

The Engineering Experiment Station was established by act of the University of Illinois Board of Trustees on December 8, 1903. Its purpose is to conduct engineering investigations that are important to the industrial interests of the state.

The management of the Station is vested in an Executive Staff composed of the Director, the Associate Director, the heads of the departments in the College of Engineering, the professor in charge of Chemical Engineering, and the Director of Engineering Information and Publications. This staff is responsible for establishing the general policies governing the work of the Station. All members of the College of Engineering teaching staff are encouraged to engage in the scientific research of the Station.

To make the results of its investigations available to the public, the Station publishes a series of bulletins. Occasionally it publishes circulars which may contain timely information compiled from various sources not readily accessible to the Station clientele or may contain important information obtained during the investigation of a particular research project but not having a direct bearing on it. A few reprints of articles appearing in the technical press and written by members of the staff are also published.

In ordering copies of these publications reference should be made to the Engineering Experiment Station Bulletin, Circular, or Reprint Series number which is at the upper left hand corner on the cover. Address

ENGINEERING PUBLICATIONS OFFICE
114 CIVIL ENGINEERING HALL
UNIVERSITY OF ILLINOIS
URBANA, ILLINOIS